

**Inducing isolated-desynchronization states in complex network of coupled chaotic oscillators**Weijie Lin,<sup>1,2</sup> Huiyan Li,<sup>3</sup> Heping Ying,<sup>2</sup> and Xingang Wang<sup>1,\*</sup><sup>1</sup>*School of Physics and Information Technology, Shaanxi Normal University, Xi'an 710062, China*<sup>2</sup>*Department of Physics, Zhejiang University, Hangzhou 310027, China*<sup>3</sup>*School of Science, Beijing University of Posts and Communications, Beijing 100876, China*

(Received 28 December 2015; revised manuscript received 21 September 2016; published 8 December 2016)

In a recent study about chaos synchronization in complex networks [Nat. Commun. **5**, 4079 (2014)], it is shown that a stable synchronous cluster may coexist with vast asynchronous nodes, resembling the phenomenon of a chimera state observed in a regular network of coupled periodic oscillators. Although of practical significance, this new type of state, namely, the isolated-desynchronization state, is hardly observed in practice due to its strict requirements on the network topology. Here, by the strategy of pinning coupling, we propose an effective method for inducing isolated-desynchronization states in symmetric networks of coupled chaotic oscillators. Theoretical analysis based on eigenvalue analysis shows that, by pinning a group of symmetric nodes in the network, there exists a critical pinning strength beyond which the group of pinned nodes can completely be synchronized while the unpinned nodes remain asynchronous. The feasibility and efficiency of the control method are verified by numerical simulations of both artificial and real-world complex networks with the numerical results in good agreement with the theoretical predictions.

DOI: [10.1103/PhysRevE.94.062303](https://doi.org/10.1103/PhysRevE.94.062303)**I. INTRODUCTION**

An intriguing dynamical pattern observed in spatiotemporal systems of coupled oscillators is the coexistence of coherent and incoherent behaviors in spatially separated domains, namely, the chimera state. This peculiar pattern was first observed and analyzed by Kuramoto and Battogtokh in simulating the complex Ginzburg-Landau equation with nonlocal couplings [1] and the later revisited and named chimera state by Abrams and Strogatz [2]. For its implications to the functioning and operation of some realistic systems, e.g., the unihemispheric sleep of dolphins and birds [3], chimera and chimeralike states have been studied extensively in the past years [4–11]. By a ring of phase oscillators coupled with a cosine kernel, an exact solution of the chimera state has been given [2], and, by a minimal model consisting of two interacting populations of oscillators, the stability and bifurcations of the chimera state have been analyzed [5]. Besides the original model of regularly coupled phase oscillators, chimera states have also been reported in other types of systems, including employing different oscillating dynamics (e.g., the periodic and chaotic maps, the Stuart-Landau oscillator, and the Hindmarsh-Rose oscillator [12–15]), different coupling functions (e.g., the time-delay and multichannel couplings [6,16]), and different network structures (e.g., the two-dimensional lattices and even the complex networks [11,17]). Meanwhile, in characterizing chimera states, many new properties have been revealed, e.g., the Brownian motion of the coherent region [7], the transient feature of the chimera pattern [18], the existence of multiple coherent regions [9,19], and the coherence-resonance chimeras [20]. Experimentally, chimera states have successfully been generated in chemical, electronic, and optical systems [21–23]. Recently, the control of chimera states has also attracted certain attention [24–26].

In exploring the collective behaviors of coupled oscillators, another interesting phenomenon is that under certain circumstances the oscillators can be self-organized into different synchronous clusters, e.g., the state of cluster (group) synchronization [27–30]. In cluster synchronization, the motions of the oscillators within the same cluster are highly correlated, whereas they are weakly or not correlated if the oscillators belong to different clusters [29]. Recently, the study of cluster synchronization has been extended to networks of complex structures in which some new phenomena have been reported [31–35]. In particular, Pecora *et al.* studied cluster synchronization in symmetric complex networks and found the interesting phenomenon of isolated desynchronization. Different from cluster synchronization where nodes are synchronized into different clusters, in isolated desynchronization a synchronous cluster emerges on the background of a large number of desynchronized nodes [35]. That is, the synchronous cluster is coexisting with the asynchronous nodes. This phenomenon is analogous to the chimera state observed in regular networks of coupled phase oscillators and, as pointed out in Ref. [35], has important implications for the functioning and security of many realistic systems, e.g., the security of the power-grid network. Yet, comparing to cluster synchronization, isolated desynchronization is much more difficult to be generated due to its strict requirements on the network topology [36]. Considering the importance of isolated desynchronization for the functioning of realistic systems, a natural question therefore is whether isolated desynchronization can be induced from an asynchronous complex network by some control methods.

In the present paper, we propose an effective control method for inducing isolated desynchronization in complex networks of coupled chaotic oscillators. Specifically, pinning a set of symmetric nodes in the network by an external controller, we are able to make only the set of pinned nodes synchronized while keeping the remaining nodes still asynchronous. We will present our control method in Sec. II, together with a theoretical analysis on the stability of the isolated-desynchronization state. In particular, based on the

\*wangxg@snnu.edu.cn

method of eigenvalue analysis, we will derive the necessary conditions for generating isolated desynchronization and give explicitly the formula of the critical pinning strength. In Sec. III, we will test the proposed method on different network models, including a small-size artificial network, the Nepal power-grid network, and a large-size complex network. For all the tested models, isolated-desynchronization states can successfully be induced, and the critical pinning strengths obtained in numerical simulations are in good agreement with the theoretical predications. Finally, we will give our discussions and conclusion in Sec. IV.

## II. CONTROL METHOD AND THEORETICAL ANALYSIS

Our model of the complex network of coupled chaotic oscillators reads

$$\dot{\mathbf{x}}_i = \mathbf{F}(\mathbf{x}_i) + \varepsilon \sum_{j=1}^N w_{ij} \mathbf{H}(\mathbf{x}_j), \quad (1)$$

with  $i, j = 1, 2, \dots, N$  as the oscillator (node) indices,  $\mathbf{x}_i$  as the state vector associated with the  $i$ th oscillator, and  $\varepsilon$  as the uniform coupling strength.  $\dot{\mathbf{x}} = \mathbf{F}(\mathbf{x})$  describes the local dynamics of the oscillators, which presents the chaotic motion and, for the sake of simplicity, is set as identical over the network.  $\mathbf{H}(\mathbf{x})$  represents the coupling function. The structural connectivity of the network is captured by the coupling matrix  $\mathbf{W} = \{w_{ij}\}$  with  $w_{ij} > 0$  as the coupling strength that node  $i$  receives from node  $j$ . If nodes  $i$  and  $j$  are not directly connected, we set  $w_{ij} = w_{ji} = 0$ . The diagonal elements of  $\mathbf{W}$  are set as  $w_{ii} = -\sum_{j, j \neq i} w_{ij}$  so as to make  $\mathbf{W}$  a Laplacian matrix [making the synchronization state a solution of Eq. (1)]. This model of linearly coupled chaotic oscillators has widely been adopted in literature for exploring the collective behaviors of networked systems. In particular, the stability of the global synchronization state can be analyzed well by the method of master stability function (MSF) [37–39], which indicates that the synchronizability of a network is jointly determined by factors, such as the network structure, the nodal dynamics, and the coupling function.

We first describe how to identify the set of nodes supporting potentially a synchronous cluster, based on the information of network symmetries [35,40–42]. Let  $i$  and  $j$  be a pair of nodes in the network whose permutation (exchange) does not change the system dynamics [i.e., the set of equations described by Eq. (1)], we call  $(i, j)$  a symmetric pair and characterize it by the permutation symmetry  $g_{ij}$ . Scanning over all the node pairs in the network, we are able to identify the whole set of permutation symmetries  $\{g_{ij}\}$ , which forms the symmetry group  $G$ . Each symmetry  $g$  can further be characterized by a permutation matrix  $\mathbf{R}_g$  with  $r_{ij} = r_{ji} = 1$  if  $i$  and  $j$  form a symmetric pair and  $r_{ij} = r_{ji} = 0$  otherwise. (For the asymmetric nodes  $r_{ii} = 1$  and  $r_{ij} = 0$  for  $i \neq j$ .)  $\mathbf{R}_g$  is commutative with the coupling matrix, i.e.,  $\mathbf{R}_g \mathbf{W} = \mathbf{W} \mathbf{R}_g$ , and, after operating on  $\mathbf{W}$ , it only exchanges the indices of nodes  $i$  and  $j$ . The set of permutation symmetries for a complex network in general is huge but can be obtained from  $\mathbf{W}$  by the technique of computational group theory [43]. Having obtained the symmetry group  $G$ , we then can partition the network nodes into different clusters according to their

permutation orbits, i.e., the subset of nodes permuting among one another through the permutation operations in group  $G$  are grouped into the same cluster. In such a way, the network nodes will be grouped into  $M$  clusters. Assuming that the network is initially staying on the fully desynchronized state (i.e., no synchronization is established between any pair of the nodes), our main objective in the present paper is to make one of the  $M$  clusters synchronized, whereas, in the meantime, keeping the remaining nodes still asynchronous.

Our method for inducing isolated desynchronization is the following. First, we select from  $M$  clusters the one we want to induce synchronization, e.g., the  $l$ th cluster which contains  $n$  nodes. We denote the set of nodes in cluster  $l$  as  $V_l$ , and by reordering the network nodes, label them with the new index  $i \in [N - n + 1, N]$ . Then, we pin all oscillators in cluster  $l$  by an external controller. The controller has exactly the same nodal dynamics and coupling function as oscillators in the network but is coupled to the oscillators in cluster  $l$  unidirectionally (i.e., the states of the oscillators in cluster  $l$  are affected by the controller but not vice versa). Finally, we increase the pinning strength and check whether and when the desired isolated-desynchronization state will be generated. Under the pinning control, the dynamics of the oscillators reads

$$\dot{\mathbf{x}}_i = \mathbf{F}(\mathbf{x}_i) + \varepsilon \sum_{j=1}^N w_{ij} \mathbf{H}(\mathbf{x}_j) + \varepsilon \eta \delta_l [\mathbf{H}(\mathbf{x}^T) - \mathbf{H}(\mathbf{x}_i)], \quad (2)$$

with  $\eta$  as the normalized pinning strength,  $\mathbf{x}^T$  as the state of the controller, and  $\delta$  as the  $\delta$  function:  $\delta_i = 1$  if  $i \in V_l$  and  $\delta_i = 0$  otherwise (i.e., only oscillators in cluster  $l$  are pinned). Equation (2) describes the general scheme of pinning control, which has extensively been used in literature for controlling the collective behaviors of coupled complex systems [44–47]. The specific questions we are interested in and going to address in the following are as follows: Can isolated desynchronization be induced by such a control method? And, if yes, what is the necessary pinning strength?

As nodes within cluster  $l$  are commutative with each other (either directly or through a permutation orbit), the isolated-desynchronization state is naturally a solution of Eq. (1). That is, if we set the initial conditions of all oscillators inside cluster  $l$  to be identical (the initial conditions of the other oscillators are still randomly chosen), then during the process of network evolution, the states of these oscillators will be always identical since they are receiving the same coupling signals from other oscillators in the network. This artificially created isolated-desynchronization state, however, is unstable due to the asynchronous nature of the network. When pinnings are added, the system dynamics will be governed by Eq. (2), and the unstable isolated-desynchronization state (which is still a solution of the system dynamics) could be stabilized when the pinning strength is larger for some threshold value. In what follows, we will conduct a theoretical analysis on this critical pinning strength, based on the method of eigenvalue analysis. Assume that the network is initially staying at the isolated-desynchronization state  $\mathbf{X} = \mathbf{X}^{\text{dsy}} \oplus \mathbf{X}^{\text{sy}}$  with  $\mathbf{X}^{\text{dsy}} = [\mathbf{x}_1, \mathbf{x}_2, \dots, \mathbf{x}_{N-n}]^T$  and  $\mathbf{X}^{\text{sy}} = [\mathbf{x}_{N-n+1}, \mathbf{x}_{N-n+2}, \dots, \mathbf{x}_N]^T$  as the state vectors of the asynchronous and synchronous oscillators, respectively. According to the definition of the isolated-desynchronization state, we have  $\mathbf{x}_i = \mathbf{x}^s$  for  $i \in V_l$

( $\mathbf{x}^s$  is the synchronous state of the oscillators in cluster  $l$ ) and  $\mathbf{x}_j \neq \mathbf{x}_{j'} \neq \mathbf{x}^s$  for  $j, j' \notin V_l$ . To investigate the stability of this state under pinning, we add infinitesimal perturbations  $\Delta \mathbf{X} = [\delta \mathbf{x}_1, \delta \mathbf{x}_2, \dots, \delta \mathbf{x}_N]^T$  on  $\mathbf{X}$  and then check the evolution of these perturbations. In the linearized form, the evolutions of the perturbations are governed by the set of variational equations,

$$\delta \dot{\mathbf{x}}_i = \mathbf{D}\mathbf{F}(\mathbf{x}_i)\delta \mathbf{x}_i + \varepsilon \sum_{j=1}^N c_{ij} \mathbf{D}\mathbf{H}(\mathbf{x}_j)\delta \mathbf{x}_j, \quad (3)$$

with  $\mathbf{D}\mathbf{F}(\mathbf{x}_i)$  and  $\mathbf{D}\mathbf{H}(\mathbf{x}_i)$  as the Jacobian matrices evaluated on the state of the  $i$ th oscillator and  $\mathbf{C}$  as the controlling matrix:  $c_{ii} = w_{ii} - \eta$  for  $i \in V_l$  (i.e., the set of nodes inside cluster  $l$ ) and  $c_{ij} = w_{ij}$  otherwise. Please note that Eq. (3) is obtained by linearizing Eq. (2) around the isolated desynchronization state  $\mathbf{X}$  instead of the global synchronization manifold used in the traditional MSF method. That is, the reference states of the oscillators inside cluster  $l$  are identical, whereas they are different from each other for oscillators not belonging to cluster  $l$ .

Let  $\mathbf{R}$  be the permutation matrix associated with the nodes in cluster  $l$  ( $r_{ij} = r_{ji} = 1$  if  $i$  and  $j$  belong to  $V_l$ ,  $r_{kk} = 1$  for  $k \notin V_l$  and  $r = 0$  for other elements) and  $\mathbf{T}$  be the transformation matrix of  $\mathbf{R}$  (i.e.,  $\mathbf{T}^{-1}\mathbf{R}\mathbf{T} = \mathbf{R}'$  with  $\mathbf{R}'$  as the diagonal matrix), then, transforming Eq. (3) into the mode space spanned by the eigenvectors of  $\mathbf{R}$ , we have the new variational equation,

$$\delta \dot{\mathbf{y}}_i = \sum_{j=1}^N \phi_{ij}(\mathbf{X})\delta \mathbf{y}_j + \varepsilon \sum_{j=1}^N c'_{ij} \sum_{k=1}^N \psi_{jk}(\mathbf{X})\delta \mathbf{y}_k, \quad (4)$$

where  $\Delta \mathbf{Y} = \{\delta \mathbf{y}_i\} = \mathbf{T}^{-1}\Delta \mathbf{X}$  is the system state in the new space,  $\mathbf{C}' = \{c'_{ij}\} = \mathbf{T}^{-1}\mathbf{C}\mathbf{T}$  is the new coupling matrix,  $\Phi = \{\phi_{ij}\} = \mathbf{T}^{-1}\mathbf{\Gamma}\mathbf{T}$  [ $\mathbf{\Gamma}$  is a diagonal matrix with the elements  $\gamma_{ii} = \mathbf{D}\mathbf{F}(\mathbf{x}_i)$ ], and  $\Psi = \{\psi_{jk}\} = \mathbf{T}^{-1}\mathbf{\Gamma}'\mathbf{T}$  [ $\mathbf{\Gamma}'$  is another diagonal matrix with the elements  $\gamma'_{ii} = \mathbf{D}\mathbf{H}(\mathbf{x}_i)$ ]. By transforming the variational equations into the mode space, a significant advantage is that the transverse space of the pinned cluster can successfully be decoupled from the others, making the stability analysis largely simplified. Specifically, in the mode space the matrix  $\mathbf{C}'$  has the blocked form

$$\mathbf{C}' = \begin{pmatrix} \mathbf{B} & \mathbf{0} \\ \mathbf{0} & \mathbf{D} \end{pmatrix}, \quad (5)$$

with  $\mathbf{B}$  and  $\mathbf{D}$  as the  $(n-1)$ - and  $(N-n+1)$ -dimensional matrices, respectively. The matrix  $\mathbf{B}$  characterizes the perturbations transverse to the synchronous manifold of cluster  $l$ , we thus name the space it spans the transverse subspace. (Please note that as  $\mathbf{C}'$  and  $\mathbf{C}$  are similar matrices, they have the same set of eigenvalues. By the transformation operation, the eigenvalues are divided into two different groups: one for matrix  $\mathbf{B}$  and the other one for matrix  $\mathbf{D}$ .) As the transverse modes are decoupled from the other modes, the synchronizability of the pinned cluster therefore can be analyzed separately. Focusing on only the transverse modes of cluster  $l$ , we have the variational equations,

$$\delta \dot{\mathbf{y}}_{i'} = \mathbf{D}\mathbf{F}(\mathbf{x}^s)\delta \mathbf{y}_{i'} + \varepsilon \sum_{j'=1}^{n-1} b_{i'j'} \mathbf{D}\mathbf{H}(\mathbf{x}^s)\delta \mathbf{y}_{j'}, \quad (6)$$

with  $i', j' = 1, 2, \dots, n-1$  as the transverse modes,  $\mathbf{B} = \{b_{i'j'}\}$ , and  $\mathbf{x}^s$  as the synchronous manifold of the pinned

cluster. Comparing to Eq. (6), Eq. (4) is significantly simplified, not only for the reduced dimension, but also because all the variational equations have the same reference state, i.e., the synchronous manifold  $\mathbf{x}^s$ .

To make the pinned cluster synchronizable, it is necessary that  $\delta \mathbf{y}_i$  should be damping to 0 with time for all the transverse modes—a question that can be addressed by the MSF method [37–39]. To be specific, transforming Eq. (6) into the mode space spanned by the eigenvectors of matrix  $\mathbf{B}$ , the variational equations of Eq. (6) can further be decoupled as

$$\delta \dot{\mathbf{z}}_{i'} = [\mathbf{D}\mathbf{F}(\mathbf{x}^s) + \varepsilon \lambda_{i'} \mathbf{D}\mathbf{H}(\mathbf{x}^s)]\delta \mathbf{z}_{i'}, \quad (7)$$

where  $0 > \lambda_1 \geq \lambda_2 \geq \dots \geq \lambda_{n-1}$  are the eigenvalues of  $\mathbf{B}$  and  $\delta \mathbf{z}_{i'}$  is the  $i'$ th perturbation mode in this new space. To make the cluster synchronizable, the necessary conditions now become that  $\delta \mathbf{z}_{i'}$  should approach 0 with time. Let  $\Lambda_{i'}$  be the largest Lyapunov exponent calculated from Eq. (7), then whether  $\delta \mathbf{z}_{i'}$  is damping with time can be determined by the sign of  $\Lambda_{i'}$ : The mode is stable if  $\Lambda_{i'} \leq 0$  and is unstable if  $\Lambda_{i'} > 0$ . Defining  $\sigma \equiv -\varepsilon \lambda$  by solving Eq. (7) numerically, we can obtain the function  $\Lambda = \Lambda(\sigma)$ , i.e., the MSF curve. Previous studies of the MSF have shown that, for the typical nonlinear oscillators,  $\Lambda$  is negative when  $\sigma$  is larger than some critical threshold  $\sigma_c$  with  $\sigma_c > 0$  as a parameter dependent on both the oscillator dynamics and the coupling function [37–39]. Hence, to keep the pinned cluster synchronizable, it is necessary that  $\sigma_{i'} > \sigma_c$  for all the transverse modes. Since  $\lambda_1 \geq \lambda_2 \geq \dots \geq \lambda_{n-1}$ , this requirement thus can be simplified as

$$\varepsilon |\lambda_1| > \sigma_c. \quad (8)$$

Since  $\mathbf{B}$  is derived from  $\mathbf{C}$  while  $\mathbf{C}$  is dependent on both the network coupling matrix  $\mathbf{W}$  and the pinning strength  $\eta$ ,  $\lambda_1$  thus is determined jointly by  $\mathbf{W}$  and  $\eta$ . To have the formula for the critical pinning strength, we need to express  $\lambda_1$  as a function of  $\eta$  explicitly. Noticing that  $\mathbf{C}$  is constructed from  $\mathbf{W}$  by replacing  $w_{ii}$  with  $w_{ii} - \eta$  for only the pinned oscillators,  $\mathbf{W}$  therefore can also be transformed into the blocked form depicted in Eq. (5) by the same transformation matrix  $\mathbf{T}$ , i.e.,  $\mathbf{W}' = \mathbf{T}^{-1}\mathbf{W}\mathbf{T}$  with  $\mathbf{W}'$  as the diagonal matrix. Denoting  $\mathbf{B}^w$  as the transverse subspace of  $\mathbf{W}'$  and letting  $0 > \lambda_1^w \geq \lambda_2^w \geq \dots \geq \lambda_{n-1}^w$  be the eigenvalues of  $\mathbf{B}^w$ , it is straightforward to find that  $\lambda_{i'} = \lambda_{i'}^w - \eta$  for  $i' = 1, 2, \dots, n-1$ . In particular, we have  $\lambda_1 = \lambda_1^w - \eta$  for the first transverse mode, which, inserting into Eq. (8), gives

$$\eta_c = \sigma_c / \varepsilon - |\lambda_1^w|. \quad (9)$$

Equation (9) is our main theoretical result, which predicts the critical pinning strength necessary for inducing synchronization for any cluster in an asynchronous network, based on only the information of the network topology, i.e., the matrix  $\mathbf{W}$ .

### III. APPLICATIONS

We next check the feasibility and efficiency of the proposed control method by applying it to different complex network models, including a small-size network, the Nepal power grid, and a large-size random network.

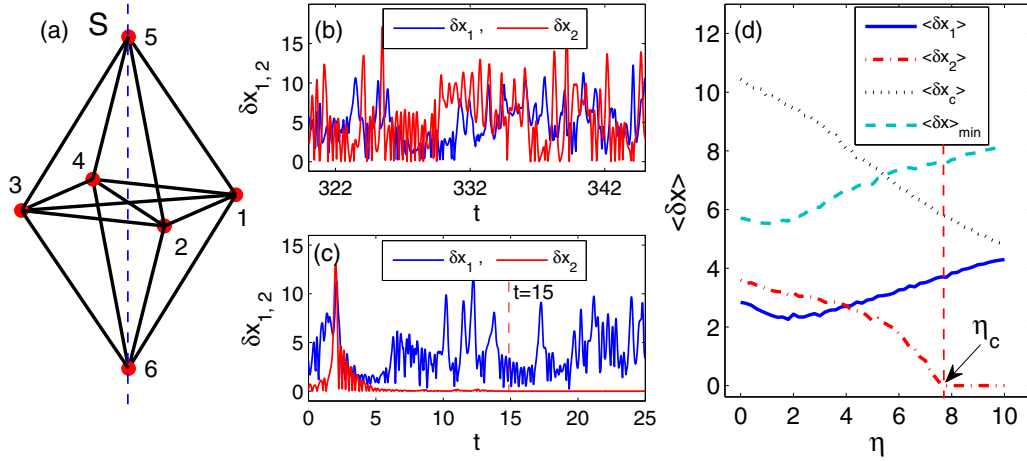


FIG. 1. Inducing isolated desynchronization from a six-node asynchronous network of coupled chaotic Lorenz oscillators. (a) The network structure. Nodes are grouped into two clusters according to their symmetries:  $V_1 = \{1-4\}$  (rotation symmetry) and  $V_2 = \{5,6\}$  (reflection symmetry). (b) By the coupling strength  $\varepsilon = 0.7$  the time evolution of the cluster-synchronization errors  $\delta x_{1,2}$  in the absence of the pinning control. Both clusters are asynchronous. (c) With the pinning strength  $\eta = 8.0$  the time evolutions of  $\delta x_{1,2}$ . Cluster 2 is synchronized at about  $t = 15$ , whereas cluster 1 remains asynchronous throughout the process. (d) The variation of the time-averaged cluster-synchronization errors  $\langle \delta x_{1,2} \rangle$  as a function of  $\eta$ .  $\langle \delta x_2 \rangle \approx 0$  at  $\eta_c \approx 7.8$ .  $\langle \delta x_c \rangle$  is the time-averaged synchronization error between oscillator 5 and the controller;  $\langle \delta x \rangle_{\min}$  is the smallest synchronization error between oscillator 5 and oscillators in cluster 1.

### A. Small-size network

We first demonstrate how to induce the isolated-desynchronization state in a small-size network. The structure of the network is presented in Fig. 1(a), which is constructed by deleting one link (e.g.,  $w_{56} = 0$ ) from a globally connected network of  $N = 6$  nodes. For the sake of simplicity, we treat the network links as nonweighted and nondirected, e.g.,  $w_{ij} = w_{ji} = 1$  for the existing links. In simulations, we adopt the chaotic Lorenz oscillator as the nodal dynamics, which in the isolated form is described by the equation  $(dx/dt, dy/dt, dz/dt)^T = [\alpha(y - x), rx - y - xz, xy - bz]^T$ . The parameters of the Lorenz oscillator are as follows:  $\alpha = 10$ ,  $r = 35$ , and  $b = 8/3$  with which the isolated oscillator shows chaotic motion with the largest Lyapunov exponent of about 1.05. The coupling function is chosen as  $\mathbf{H}([x, y, z]^T) = [0, x, 0]^T$ . Having fixed the nodal dynamics and coupling function, we then can obtain the MSF curve  $\Lambda = \Lambda(\sigma)$  by solving Eq. (7) numerically, which shows that  $\Lambda < 0$  for  $\sigma > \sigma_c \approx 8.3$  [39].

For this simple network, the network symmetries can be discerned by visual inspection: The group of nodes (1–4) is of rotation symmetry, and the pair of nodes (5,6) is of reflection symmetry. Accordingly, the nodes can be divided into two clusters:  $V_1 = \{1-4\}$  and  $V_2 = \{5,6\}$ . To measure the synchronization degree of the clusters, we introduce the cluster-synchronization error  $\delta x_l = \sum_{i=1}^{n_l} |x_i - \bar{x}_l| / n_l$  with  $i \in V_l$ ,  $n_l$  as the number of nodes in cluster  $l$  and  $\bar{x}_l = \sum_i x_i / n_l$  as the cluster-averaged state. Clearly, the smaller the  $\delta x_l$ , the better the oscillators within cluster  $l$  are synchronized. Setting  $\varepsilon = 0.7$ , we plot in Fig. 1(b) the evolutions of  $\delta x_1$  and  $\delta x_2$  as a function of time. It is shown that neither of the clusters is synchronized. To implement the control method, we pin oscillators 5 and 6 by an external controller according to Eq. (2) so as to induce synchronization solely for oscillators in cluster 2. (It is worth noting that, due to the network

topology, this cluster cannot be synchronized by varying the coupling strength, i.e., it is topologically unstable. In contrast, the first cluster could be synchronized when the coupling strength is larger for some critical value, i.e., it is dynamically unstable [36].) By the pinning strength  $\eta = 8.0$ , in Fig. 1(c) we plot again the time evolutions of  $\delta x_1$  and  $\delta x_2$ . It is seen that, after a transient period of about  $t = 15$ , we have  $\delta x_2 \approx 0$ , whereas  $\delta x_1$  is still of large values. Indeed, with the pinning control, the desired isolated-desynchronization state can be induced from the asynchronous network.

To identify the critical pinning strength  $\eta_c$  for inducing the desired isolated-desynchronization state, we plot in Fig. 1(d) the variation of the time-averaged cluster-synchronization error (which is averaged over a period of length  $t = 50$  after discarding a transient period of length  $t = 100$ )  $\langle \delta x_l \rangle$  as a function of  $\eta$ . It is seen that  $\langle \delta x_2 \rangle$  reaches 0 about 7.8, whereas  $\langle \delta x_1 \rangle$  remains at large values. We thus have  $\eta_c \approx 7.8$  numerically. To check whether synchronization is achieved between the controller and the pinned oscillators too, we also plot in Fig. 1(d) the variation of the time-averaged synchronization error between oscillator 5 and the controller  $\langle \delta x_c \rangle = \langle |x_5 - x^T| \rangle$  as a function of  $\eta$ . It is seen that  $\langle \delta x_c \rangle$  remains large for  $\eta > \eta_c$ , indicating that the synchronous cluster is induced but not controlled by the external controller. (In our simulations, we have increased  $\eta$  up to 30 and found that the value of  $\langle \delta x_c \rangle$  is still large.) Meanwhile, to check whether there are other synchronous clusters formed in the network, we also plot in Fig. 1(d) the variation of the smallest synchronization error between oscillators in cluster 1 and oscillator 5  $\langle \delta x \rangle_{\min} = \min\{|x_5 - x_j|\}$  with  $j \in V_1$ . As  $\langle \delta x \rangle_{\min} > 0$  in the region  $\eta > \eta_c$ , the possibility of forming other synchronous clusters thus is excluded.

The critical pinning strength for inducing the isolated-desynchronization state  $\eta_c$  can be analyzed by the method of eigenvalue analysis presented in Sec. II as follows. As nodes 5 and 6 satisfy the reflection symmetry, their permutation

does not change the system dynamics. We therefore have the permutation matrix,

$$\mathbf{R} = \begin{pmatrix} 1 & 0 & 0 & 0 & 0 & 0 \\ 0 & 1 & 0 & 0 & 0 & 0 \\ 0 & 0 & 1 & 0 & 0 & 0 \\ 0 & 0 & 0 & 1 & 0 & 0 \\ 0 & 0 & 0 & 0 & 0 & 1 \\ 0 & 0 & 0 & 0 & 1 & 0 \end{pmatrix}, \quad (10)$$

from which we can obtain the transformation matrix (constructed by the eigenvectors of  $\mathbf{R}$ ),

$$\mathbf{T} = \begin{pmatrix} 0 & 0 & 0 & 0 & 1 & 0 \\ 0 & 1 & 0 & 0 & 0 & 0 \\ 0 & 0 & 1 & 0 & 0 & 0 \\ 0 & 0 & 0 & 1 & 0 & 0 \\ -\sqrt{2}/2 & 0 & 0 & 0 & 0 & \sqrt{2}/2 \\ \sqrt{2}/2 & 0 & 0 & 0 & 0 & \sqrt{2}/2 \end{pmatrix}. \quad (11)$$

As nodes 5 and 6 are pinned by the controller, we have the controlling matrix,

$$\mathbf{C} = \begin{pmatrix} -5 & 1 & 1 & 1 & 1 & 1 \\ 1 & -5 & 1 & 1 & 1 & 1 \\ 1 & 1 & -5 & 1 & 1 & 1 \\ 1 & 1 & 1 & -5 & 1 & 1 \\ 1 & 1 & 1 & 1 & -4 - \eta & 0 \\ 1 & 1 & 1 & 1 & 0 & -4 - \eta \end{pmatrix}, \quad (12)$$

which, after the transformation operation  $\mathbf{C}' = \mathbf{T}^{-1}\mathbf{C}\mathbf{T}$ , has the blocked form shown in Eq. (5) with

$$\mathbf{D} = \begin{pmatrix} -5 & 1 & 1 & 1 & \sqrt{2} \\ 1 & -5 & 1 & 1 & \sqrt{2} \\ 1 & 1 & -5 & 1 & \sqrt{2} \\ 1 & 1 & 1 & -5 & \sqrt{2} \\ \sqrt{2} & \sqrt{2} & \sqrt{2} & \sqrt{2} & -4 - \eta \end{pmatrix}, \quad (13)$$

and

$$\mathbf{B} = -4 - \eta. \quad (14)$$

We thus have  $\lambda_1 = \lambda_1^w - \eta = -4 - \eta$ , which, according to Eq. (8), gives  $\eta_c = \sigma_c/\varepsilon - |\lambda_1^w| = 8.3/0.7 - 4 \approx 7.86$ . This theoretical prediction is in good agreement with the numerical result presented in Fig. 1(d) (numerically we have  $\eta_c \approx 7.8$ ).

### B. Power-grid network

We next demonstrate how to induce isolated desynchronization in a power-grid complex network. The network model employed here is the Nepal power grid [48], which contains  $N = 15$  nodes (power stations) and 62 links (power lines). For the sake of simplicity, we still treat the links as nonweighted and nondirected, e.g.,  $w = 1$  for the existing links. By the technique of computational group theory [35,43], we are able to figure out all the network permutation symmetries (totally 86 400) and, according to the permutation orbits, partition

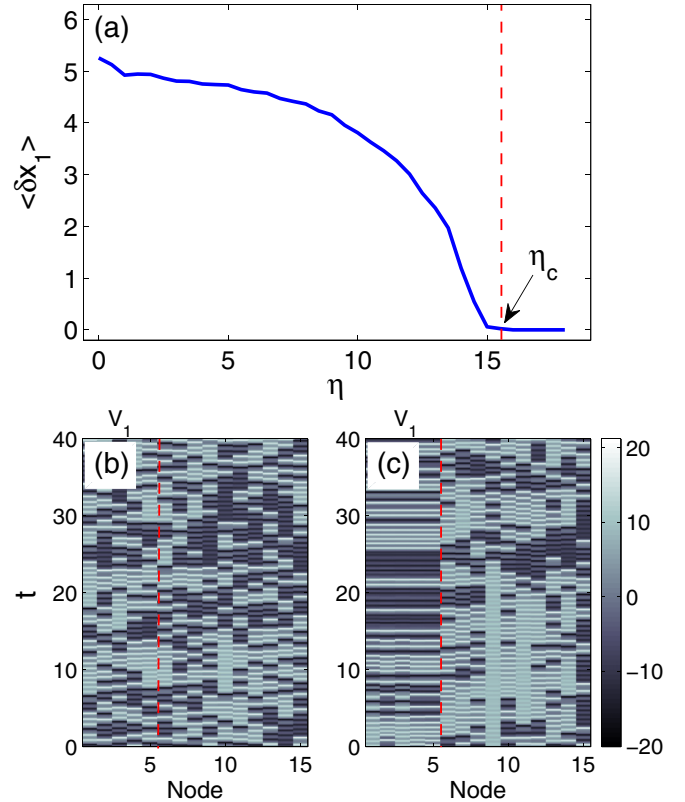


FIG. 2. Inducing isolated desynchronization in the network of the Nepal power grid. The nodal dynamics and coupling function are the same as in Fig. 1. The coupling strength is fixed as  $\varepsilon = 0.32$  with which no synchronization is established between any pair of the oscillators. Pinning control is added on oscillators in cluster 1. (a) The variation of the time-averaged synchronization error of cluster 1 ( $\langle \delta x_1 \rangle$ ) as a function of the pinning strength  $\eta$ . Isolated desynchronization is induced when  $\eta > \eta_c \approx 16$ . The spatiotemporal evolution of the oscillators under the pinning strengths (b)  $\eta = 14$  and (c)  $\eta = 18$ .

the nodes into five clusters:  $V_1 = \{1-5\}$ ,  $V_2 = \{6-8\}$ ,  $V_3 = \{9-13\}$ ,  $V_4 = \{14\}$ , and  $V_5 = \{15\}$  [35]. Among them, the fourth and fifth clusters are trivial as each contains only a single node. Still, we adopt the chaotic Lorenz oscillator as the nodal dynamics and use  $\mathbf{H}([x, y, z]^T) = [0, x, 0]^T$  as the coupling function. The coupling strength is fixed as  $\varepsilon = 0.32$  with which no synchronization is established between any pair of oscillators in the network.

For illustration purposes, we pin oscillators in cluster 1 according to Eq. (2). Based on numerical simulations, we plot in Fig. 2(a) the variation of the time-averaged synchronization error for cluster 1 ( $\langle \delta x_1 \rangle$ ) as a function of the pinning strength  $\eta$ . It is seen that  $\langle \delta x_1 \rangle$  decreases gradually as  $\eta$  increases and reaches 0 at about  $\eta_c \approx 16$ . To take a closer look at the transition of the system dynamics from the asynchronous to isolated-desynchronization states around  $\eta_c$ , we plot in Figs. 2(b) and 2(c) the spatiotemporal evolution of the network for different values of  $\eta$ . For the case of  $\eta = 14 < \eta_c$  [Fig. 2(b)], it is seen that the evolution is random and irregular through the process. For the case of  $\eta = 18 > \eta_c$  [Fig. 2(c)], it is shown that, after a transient period of about  $t \approx 18$ , the

oscillators in cluster 1 are well synchronized, whereas the other oscillators in the network remain asynchronous.

Still, the critical pinning strength  $\eta_c$ , obtained in numerical simulations [Fig. 2(a)] can be analyzed by the method of eigenvalue analysis presented in Sec. II. To save space, here we omit the detailed deductions but present only the main results. In constructing the permutation matrix  $\mathbf{R}$ , we set  $r_{ij} = r_{ji} = 1$  for  $i, j \in V_1$ ,  $r_{kk} = 1$  for  $k \notin V_1$  and  $r = 0$  for the remaining elements. By the eigenvectors of  $\mathbf{R}$ , we construct the transformation matrix  $\mathbf{T}$  and then use it to transform the control matrix  $\mathbf{C}$  into the blocked matrix  $\mathbf{C}'$  [which has the blocked form shown in Eq. (5)]. From  $\mathbf{C}'$ , we finally obtain the transverse matrix  $\mathbf{B}$ , which is four dimensional and has the degenerated eigenvalues  $\lambda_{1-4} = \lambda_1^w - \eta = -8 - \eta$ . According to Eq. (8), we thus have theoretically  $\eta_c = \sigma_c/\varepsilon - |\lambda_1^w| = 8.3/0.32 - 8 \approx 18$ . As shown in Fig. 2, this theoretical prediction is in good agreement with the numerical result (numerically we have  $\eta_c \approx 16$ ).

### C. Large-size complex network

We finally demonstrate how to induce isolated desynchronization in a large-size complex network. Recently, a new type of chimera state consisting of two or more coherent regions, namely, the multiple-cluster chimera state has been reported in regular networks of coupled periodic oscillators [9,19]. As an isolated-desynchronization state is analogous to a chimera state, it is intriguing to see whether it is possible to induce two synchronous clusters out of the asynchronous states by the proposed method. To investigate, we generate a random network of  $N = 100$  nodes and 4931 links (constructed by randomly removing 19 links from the globally connected network). Again, we adopt the chaotic Lorenz oscillator as the nodal dynamics and use  $\mathbf{H}([x, y, z]^T) = [0, x, 0]^T$  as the coupling function. This time, to avoid the overflow in numerical simulations, we adopt the normalized coupling scheme:  $w_{ij} = a_{ij}/k_i$  for the nondiagonal elements and  $w_{ii} = -1$  for the diagonal elements [49,50]. Here  $\mathbf{A} = \{a_{ij}\}$  is the adjacency matrix ( $a_{ij} = 1$  if nodes  $i$  and  $j$  are connected, otherwise  $a_{ij} = 0$ ), and  $k_i = \sum_j a_{ij}$  is the degree of node  $i$  (the number of links attached to node  $i$ ). In general, we have  $w_{ij} \neq w_{ji}$ , i.e., the couplings are weighted and directed. By the technique of computational group theory, we can find out all the network symmetries for this network, based on which the network nodes can be grouped into four clusters. In particular, the largest cluster contains 66 nodes ( $V_1 = \{1, 2, \dots, 66\}$ ), and the second largest cluster contains 22 nodes ( $V_2 = \{79, 80, \dots, 100\}$ ). We fix the coupling strength as  $\varepsilon = 4.4$  with which no synchronization is observed between any pair of oscillators in the absence of pinning control.

To implement the control, we introduce two independent external controllers  $\mathbf{x}^{T1}$  and  $\mathbf{x}^{T2}$  with controllers 1 and 2 pinning the oscillators in clusters 1 and 2, respectively. The two controllers have the same dynamics and pinning strength but are evolving independently (i.e., they are not coupled to each other). Based on numerical simulations, we plot in Fig. 3(a) the variation of the time-averaged cluster-synchronization errors  $\langle \delta x_{1,2} \rangle$  as a function of  $\eta$ . It is seen that  $\langle \delta x_1 \rangle$  and  $\langle \delta x_2 \rangle$  reach 0 at about  $\eta_{c1} \approx 0.86$  and  $\eta_{c2} \approx 0.91$ , respectively. Therefore, in the region  $\eta \in (\eta_{c1}, \eta_{c2})$  the network is staying

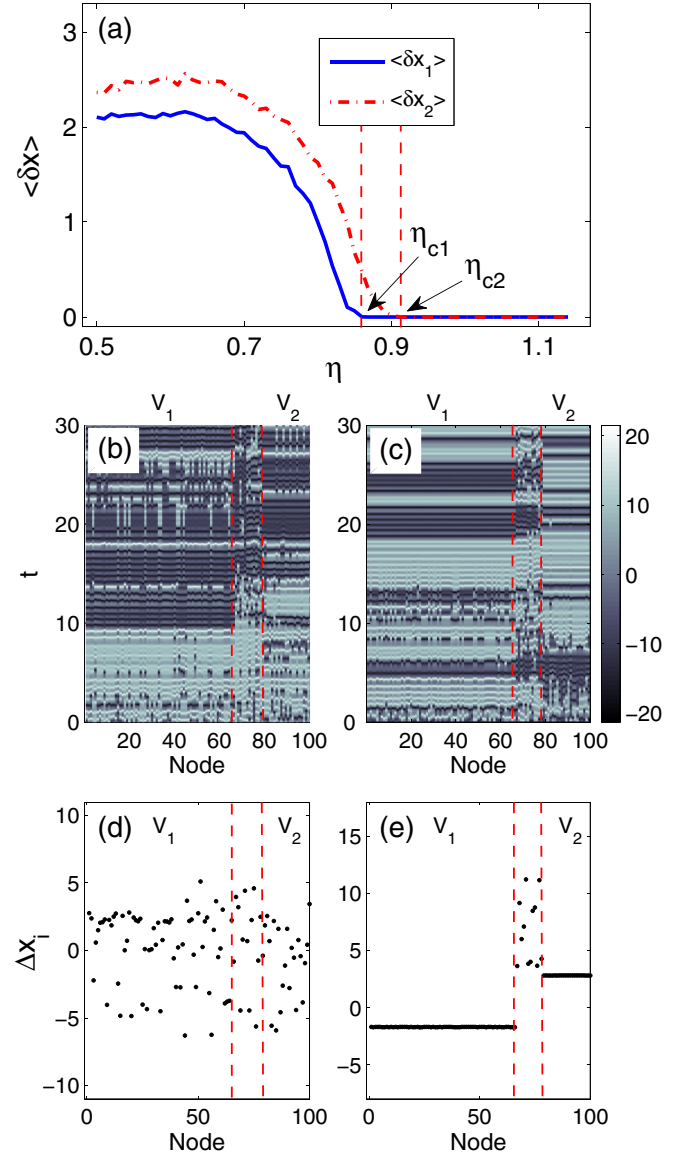


FIG. 3. Inducing the isolated-desynchronization state of two synchronous clusters in a random network of  $N = 100$  chaotic Lorenz oscillators. The coupling strength is fixed as  $\varepsilon = 4.4$  with which the network is asynchronous. (a) The variation of the time-averaged cluster-synchronization errors  $\langle \delta x_{1,2} \rangle$  as a function of the pinning strength  $\eta$ .  $\langle \delta x_1 \rangle$  and  $\langle \delta x_2 \rangle$  reach 0 at  $\eta_{c1} \approx 0.86$  and  $\eta_{c2} \approx 0.91$ , respectively. The spatiotemporal evolution of the network under the pinning strengths (b)  $\eta = 0.8$  and (c)  $\eta = 0.95$ . The snapshots of the network taken at  $t = 20$  for (d)  $\eta = 0.8$  and (e)  $\eta = 0.95$ .  $\Delta x_i = x_i - \bar{x}$  with  $\bar{x} = \sum_i x_i / N$  as the network-averaged state.

on a one-cluster isolated-desynchronization state (only cluster 1 is synchronized), and in the region  $\eta > \eta_{c2}$  the network is staying on a two-cluster isolated-desynchronization state (both clusters 1 and 2 are synchronized).

For more details on the formation of the two-cluster isolated-desynchronization state, we plot in Figs. 3(b) and 3(c) the spatiotemporal evolution of the network under different pinning strengths. For a weak pinning strength  $\eta = 0.8 < \eta_{c1}$  [Fig. 3(b)], it is seen that the oscillators are evolving

independently without any sign of synchronization for both clusters. For a strong pinning strength  $\eta = 0.95 > \eta_{c2}$  [Fig. 3(c)], it is seen clearly that the motions of the oscillators in each cluster  $V_{1,2}$  are highly correlated. To characterize further the formation of the two-cluster isolated-desynchronization state, we plot in Figs. 3(d) and 3(e) the snapshots of the network at the moment  $t = 20$  of the system evolutions presented in Figs. 3(b) and 3(c). For the case of  $\eta = 0.8$  [Fig. 3(d)], it is seen that the states of the oscillators are scattered randomly over a wide range, indicating the absence of synchronous cluster; whereas for the case of  $\eta = 0.95$  [Fig. 3(e)], the states of the oscillators in  $V_1$  ( $V_2$ ) are identical, indicating the synchronization of cluster 1 (cluster 2) is achieved.

Despite the weighted coupling matrix and the pinning for two clusters, the critical pinning strengths  $\eta_{c1}$  and  $\eta_{c2}$  can still be analyzed by the method of eigenvalue analysis proposed in Sec. II. In constructing the permutation matrix  $\mathbf{R}$ , we set  $r_{ij} = r_{ji} = 1$  if nodes  $i$  and  $j$  belong to  $V_1$  ( $V_2$ ) and  $r_{kk} = 1$  for other nodes. Transformed into the mode space of  $\mathbf{R}$ , the controlling matrix has the blocked form of Eq. (5). Different from the one-cluster case, here there are two transverse subspaces  $\mathbf{B}_1$  and  $\mathbf{B}_2$ .  $\mathbf{B}_1$  is 65 dimensional, which characterizes the transverse subspace of cluster 1. The largest eigenvalues of  $\mathbf{B}_1$  is  $\lambda_1 = \lambda_1^w - \eta = -1.01 - \eta$ , which, according to Eq. (8), gives  $\eta_{c1} = \sigma_c/\varepsilon - |\lambda_1^w| = 8.3/4.4 - 1.01 \approx 0.88$ .  $\mathbf{B}_2$  is 21 dimensional, which characterizes the transverse subspace of cluster 2. The largest eigenvalue of  $\mathbf{B}_2$  is  $\lambda_1 = \lambda_1^w - \eta = -1.0 - \eta$ , which, according to Eq. (8), gives  $\eta_{c2} = \sigma_c/\varepsilon - |\lambda_1^w| = 8.3/4.4 - 1.0 \approx 0.89$ . The theoretical predictions are in good agreement with the numerical results shown in Fig. 3 (numerically we have  $\eta_{c1} \approx 0.86$  and  $\eta_{c2} \approx 0.91$ ).

#### IV. DISCUSSIONS AND CONCLUSION

The proposed method of inducing isolated desynchronization could be applied to the general complex networks of coupled nonlinear oscillators. In our simulations, we have applied this method to a variety of complex networks (including all the network models studied in Ref. [35]) and found that, given the network contains a symmetric cluster, there always exists a critical pinning strength beyond which the desired isolated-desynchronization state can stably be generated. Meanwhile, as the underlying mechanism for generating isolated desynchronization is governed by cluster synchronization, the proposed control method might potentially be applied to a complex network of the general nodal dynamics and coupling functions. For instance, replacing the coupling function with  $\mathbf{H}[x, y, z]^T = [x, 0, 0]^T$  (different from the one demonstrated above, this coupling function generates a bounded stable region in the MSF curve), we have observed the similar isolated-desynchronization states shown in Figs. 1–3. Besides the chaotic Lorenz oscillators, we have also tested the other nodal dynamics, including the chaotic Rössler and Hindmarsh-Rose oscillators where the similar isolated-desynchronization states have successfully been induced by the proposed pinning method (results to be presented elsewhere).

It should be emphasized that the proposed pinning method is able to induce, but not control, the synchronous cluster. This

property is rooted in the symmetry of the enlarged pinning network, i.e., considering the controller as an additional node to the original network. In this enlarged network, the oscillators in the pinned cluster are still satisfying the permutation symmetry, but they are not exchangeable with the controller. As the pinned oscillators are perturbed by the desynchronized oscillators while the controller is not, it is therefore impossible to make the pinned oscillators synchronize with the controller. However, if the whole network is synchronized (instead of a few of the clusters), it would be possible to control the whole network for the manifold defined by the controller. In such a case, the whole network, the original network, and the controller, will reach the state of global synchronization instead of isolated desynchronization [46,47].

The inducing of isolated synchronization in asynchronous complex networks might have implications for the functioning and operation for some real-world systems. One example could be the functioning of the brain network where neurons are clustered into functional areas that are organized in a hierarchical fashion [51]. In realizing the high-level brain functions, such as memory and cognition, it is normally observed that, coordinated by the signals sent out from neurons at the upper level of the hierarchy, a fraction of the neurons at the lower level could be synchronized into dynamical clusters while the other neurons remain asynchronous, forming the function-related dynamical patterns (e.g., the mechanism of binding synchronization [51]). For instance, the dopamine complex in the midbrain is constituted by several functional sectors with each sector being used to coordinate the synchronous behavior of a collection of neurons in a specific functional-anatomical macrosystem of the basal forebrain [52]. Another example where isolated desynchronization is of important concern is the operating of the international (global) power grid [53,54] where the power generators of a fraction of the nations are synchronized in both frequency and phase, whereas the other nations are asynchronous. Also, from the security point of view, when a large-scale blackout occurs, and many of the power generators fail to operate synchronously, it would be desirable if the synchronization of some important generators can be reestablished by some control technique [53,54].

To summarize, we have proposed a pinning method which is able to induce synchronization for only the desired clusters, i.e., the isolated-desynchronization states, in symmetric complex networks of coupled chaotic oscillators. We have found that, given that the network contains a group of symmetric nodes, there always exists a critical pinning strength beyond which a stable synchronous cluster can be generated on the background of vast desynchronized nodes. We have conducted a detailed analysis on the stability of the isolated-desynchronization state and obtained explicitly the formula for the critical pinning strength. The feasibility and efficiency of the control method have been verified by numerical simulations of various network models with the numerical results in good agreement with the theoretical predictions. Our paper shed light on the collective dynamics of complex networks and might be helpful for our understanding on the functioning of neuronal systems as well as for the design of modern control techniques for infrastructure networks, such as the power grid.

## ACKNOWLEDGMENTS

This work was supported by the National Natural Science Foundation of China under Grant No. 11375109 and by the

Fundamental Research Funds for the Central Universities under Grant No. GK201601001.

- 
- [1] Y. Kuramoto and D. Battogtokh, Coexistence of coherence and incoherence in nonlocally coupled phase oscillators, *Nonlinear Phenom. Complex Syst.* **5**, 380 (2002).
- [2] D. Abrams and S. Strogatz, Chimera States for Coupled Oscillators, *Phys. Rev. Lett.* **93**, 174102 (2004).
- [3] M. Panaggio and D. Abrams, Chimera states: Coexistence of coherence and incoherence in networks of coupled oscillators, *Nonlinearity* **28**, R67 (2015).
- [4] A. Zakharova, M. Kapeller, and E. Schöll, Chimera Death: Symmetry Breaking in Dynamical Networks, *Phys. Rev. Lett.* **112**, 154101 (2014).
- [5] D. Abrams, R. Mirollo, S. Strogatz, and D. Wiley, Solvable Model for Chimera States of Coupled Oscillators, *Phys. Rev. Lett.* **101**, 084103 (2008).
- [6] G. Sethia, A. Sen, and F. Ataym, Clustered Chimera States in Delay-Coupled Oscillator Systems, *Phys. Rev. Lett.* **100**, 144102 (2008).
- [7] O. E. Omel'chenko, M. Wolfrum, and Y. Maistrenko, Chimera states as chaotic spatiotemporal patterns, *Phys. Rev. E* **81**, 065201(R) (2010).
- [8] S. Nkomo, M. R. Tinsley, and K. Showalter, Chimera States in Populations of Nonlocally Coupled Chemical Oscillators, *Phys. Rev. Lett.* **110**, 244102 (2013).
- [9] S. Ujjwal and R. Ramaswamy, Chimeras with multiple coherent regions, *Phys. Rev. E* **88**, 032902 (2013).
- [10] C. Lang, Chimera states in heterogeneous networks, *Chaos* **19**, 013113 (2009).
- [11] S. Shima and Y. Kuramoto, Rotating spiral waves with phase-randomized core in nonlocally coupled oscillators, *Phys. Rev. E* **69**, 036213 (2004).
- [12] I. Omelchenko, Y. Maistrenko, P. Hövel, and E. Schöll, Loss of Coherence in Dynamical Networks: Spatial Chaos and Chimera States, *Phys. Rev. Lett.* **106**, 234102 (2011).
- [13] I. Omelchenko, B. Riemenschneider, P. Hövel, Y. Maistrenko, and E. Schöll, Transition from spatial coherence to incoherence in coupled chaotic systems, *Phys. Rev. E* **85**, 026212 (2012).
- [14] C. Laing, Chimeras in networks of planar oscillators, *Phys. Rev. E* **81**, 066221 (2010).
- [15] J. Hizanidis, V. Kanas, A. Bezerianos, and T. Bountis, Chimera states in networks of nonlocally coupled Hindmarsh-Rose neuron models, *Int. J. Bifurcation Chaos* **24**, 1450030 (2014).
- [16] I. Omelchenko, O. E. Omel'chenko, P. Hövel, and E. Schöll, When Nonlocal Coupling Between Oscillators Becomes Stronger: Patched Synchrony or Multichimera States, *Phys. Rev. Lett.* **110**, 224101 (2013).
- [17] Y. Zhu, Z. Zheng, and J. Yang, Chimera states on complex networks, *Phys. Rev. E* **89**, 022914 (2014).
- [18] M. Wolfrum and O. E. Omel'chenko, Chimera states are chaotic transients, *Phys. Rev. E* **84**, 015201(R) (2011).
- [19] Y. Zhu, Y. Li, M. Zhang, and J. Yang, The oscillating two-cluster chimera state in non-locally coupled phase oscillators, *Europhys. Lett.* **97**, 10009 (2012).
- [20] N. Semenova, A. Zakharova, V. Anishchenko, and E. Schöll, Coherence-Resonance Chimeras in a Network of Excitable Elements, *Phys. Rev. Lett.* **117**, 014102 (2016).
- [21] M. Tinsley, S. Nkomo, and K. Showalter, Chimera and phase-cluster states in populations of coupled chemical oscillators, *Nat. Phys.* **8**, 662 (2012).
- [22] L. Larger, B. Penkovsky, and Y. Maistrenko, Virtual Chimera States for Delayed-Feedback Systems, *Phys. Rev. Lett.* **111**, 054103 (2013).
- [23] A. Hagerstrom, T. Murphy, R. Roy, P. Hövel, I. Omelchenko, and E. Schöll, Experimental observation of chimeras in coupled-map lattices, *Nat. Phys.* **8**, 658 (2012).
- [24] J. Sieber, O. E. Omel'chenko, and M. Wolfrum, Controlling Unstable Chaos: Stabilizing Chimera States by Feedback, *Phys. Rev. Lett.* **112**, 054102 (2014).
- [25] O. E. Omel'chenko, Y. Maistrenko, and P. Tass, Chimera states induced by spatially modulated delayed feedback, *Phys. Rev. E* **82**, 066201 (2010).
- [26] C. Bick and E. Martens, Controlling chimeras, *New J. Phys.* **17**, 033030 (2015).
- [27] M. Hasler, Y. Maistrenko, and O. Popovych, Simple example of partial synchronization of chaotic systems, *Phys. Rev. E* **58**, 6843 (1998).
- [28] Y. Zhang, G. Hu, H. Cerdeira, S. Chen, T. Braun, and Y. Yao, Partial synchronization and spontaneous spatial ordering in coupled chaotic systems, *Phys. Rev. E* **63**, 026211 (2001).
- [29] A. Pikovsky, O. Popovych, and Y. Maistrenko, Resolving Clusters in Chaotic Ensembles of Globally Coupled Identical Oscillators, *Phys. Rev. Lett.* **87**, 044102 (2001).
- [30] B. Ao and Z. Zheng, Partial synchronization on complex networks, *Europhys. Lett.* **74**, 229 (2006).
- [31] C. Zhou and J. Kurths, Hierarchical synchronization in complex networks with heterogeneous degrees, *Chaos* **16**, 015104 (2006).
- [32] X. G. Wang, S. Guan, Y.-C. Lai, B. Li, and C. H. Lai, Desynchronization and on-off intermittency in complex networks, *Europhys. Lett.* **88**, 28001 (2009).
- [33] C. Fu, Z. Deng, L. Huang, and X. G. Wang, Topological control of synchronous patterns in systems of networked chaotic oscillators, *Phys. Rev. E* **87**, 032909 (2013).
- [34] C. Fu, W. Lin, L. Huang, and X. G. Wang, Synchronization transition in networked chaotic oscillators: The viewpoint from partial synchronization, *Phys. Rev. E* **89**, 052908 (2014).
- [35] L. Pecora, F. Sorrentino, A. Hagerstrom, T. Murphy, and R. Roy, Cluster synchronization and isolated desynchronization in complex networks with symmetries, *Nat. Commun.* **5**, 4079 (2014).
- [36] W. Lin, H. Fan, Y. Wang, H. Ying, and X. G. Wang, Controlling synchronous patterns in complex networks, *Phys. Rev. E* **93**, 042209 (2016).
- [37] L. Pecora and T. Carroll, Master Stability Functions for Synchronized Coupled Systems, *Phys. Rev. Lett.* **80**, 2109 (1998).

- [38] G. Hu, J. Yang, and W. Liu, Instability and controllability of linearly coupled oscillators: Eigenvalue analysis, *Phys. Rev. E* **58**, 4440 (1998).
- [39] L. Huang, Q. Chen, Y.-C. Lai, and L. Pecora, Generic behavior of master-stability functions in coupled nonlinear dynamical systems, *Phys. Rev. E* **80**, 036204 (2009).
- [40] O. D’Huys, R. Vicente, T. Erneux, J. Danckaert, and I. Fischer, Synchronization properties of network motifs: Influence of coupling delay and symmetry, *Chaos* **18**, 037116 (2008).
- [41] G. Russo and J. J. E. Slotine, Symmetries, stability, and control in nonlinear systems and networks, *Phys. Rev. E* **84**, 041929 (2011).
- [42] M. Golubitsky and I. Stewart, Recent advances in symmetric and network dynamics, *Chaos* **25**, 097612 (2015).
- [43] W. Stein, *SAGE: Software for Algebra and Geometry Experimentation* [<http://www.sagemath.org/sage/>, 2013].
- [44] G. Hu and Z. L. Qu, Controlling Spatiotemporal Chaos in Coupled Map Lattice Systems, *Phys. Rev. Lett.* **72**, 68 (1994).
- [45] F. Sorrentino, M. Bernardo, F. Garofalo, and G. Chen, Controllability of complex networks via pinning, *Phys. Rev. E* **75**, 046103 (2007).
- [46] X. F. Wang and G. R. Chen, Pinning control of scale-free dynamical networks, *Physica A* **310**, 521 (2002).
- [47] L. Yang, X. G. Wang, Y. Li, and Z. M. Sheng, On the pinning strategy of complex networks, *Europhys. Lett.* **92**, 48002 (2010).
- [48] Nepal Electricity Authority Annual report 2011 [available at <http://www.nea.org.np>].
- [49] A. E. Motter, C. S. Zhou, and J. Kurths, Enhancing complex-network synchronization, *Europhys. Lett.* **69**, 334 (2005).
- [50] X. G. Wang, Y.-C. Lai, and C.-H. Lai, Enhancing synchronization based on complex gradient networks, *Phys. Rev. E* **75**, 056205 (2007).
- [51] E. Basar, *Brain Function and Oscillation* (Springer, New York, 1998).
- [52] L. Yetnikoff, H. N. Lavezzi, R. A. Reichard, and D. S. Zahm, An update on the connections of the ventral mesencephalic dopaminergic complex, *Neuroscience* **282**, 23 (2014).
- [53] M. Z. Jacobson and M. A. Delucchi, Providing all global energy with wind, water, and solar power, Part I: Technologies, energy resources, quantities and areas of infrastructure, and materials, *Energy Policy* **39**, 1154 (2011).
- [54] S. Chatzivasileiadis, D. Ernst, and G. Andersson, The global grid, *Renewable Energy* **57**, 372 (2013).